Supporting Information

Combined Multi-modal Optical Imaging and Targeted Gene Silencing Using Stimuli-transforming Nanotheragnostics

Min Suk Shim[†], Chang Soo Kim[†,‡], Yeh-Chan Ahn[‡], Zhongping Chen[†,‡,§], and Young Jik Kwon*[,†,§,∥]

[†]Department of Chemical Engineering and Materials Science, University of California, Irvine, CA 92697, [‡]Beckman Laser Institute, University of California, Irvine, CA 92612, [§]Department of Biomedical Engineering, University of California, Irvine, CA 92697, [∥]Pharmaceutical Sciences, University of California, Irvine, CA 92697

Setup of spectral domain (SD) optical coherence tomography (OCT)

SD-OCT (Figure S1) was used to quantify the scattering intensity and the Doppler variance of the nanoparticles before and after hydrolysis. Using the phase-resolved method, the scattering intensity *I*, the mean Doppler frequency shift $\overline{\omega}$, and the Doppler variance σ^2 can be determined from the depth encoded complex signal *f*(*z*, *t*) as shown in equations (Eq. S1-3) [1, 2]. The depth encoded complex signal *f*(*z*, *t*) can be obtained by taking the inverse Fourier transformation of camera fringe in wave number domain [3]:

$$I(z,t) = \left| f(z,t) \right| \qquad \text{Eq. S1}$$

$$\overline{\omega}(z,t) = \frac{1}{T}\tan^{-1}\left\{ \frac{\mathrm{Im}\left(\sum_{j=0}^{N-1} \left[f(z,t+(j+1)T) \cdot f^*(z,t+jT) \right] \right)}{\mathrm{Re}\left(\sum_{j=0}^{N-1} \left[f(z,t+(j+1)T) \cdot f^*(z,t+jT) \right] \right)} \right\} (\mathrm{rad}) \qquad \text{Eq. S2}$$

$$\sigma^2(z,t) = \frac{2}{T^2}\left\{ 1 - \frac{\left| \sum_{j=0}^{N-1} \left[f(z,t+(j+1)T) \cdot f^*(z,t+jT) \right] \right|}{\sum_{j=0}^{N-1} \left[f(z,t+jT) \cdot f^*(z,t+jT) \right]} \right\} (\mathrm{rad}^2) \qquad \text{Eq. S3}$$

where *z* is the depth, *t* is the time, * denotes the complex conjugate, *T* is the time between two consecutive camera exposures, and *N* is the number of ensemble averages. The source arm has a

broadband light source, which has a center wavelength of 1310 nm and a full width at half maximum (FWHM) of 90 nm. Frame rate of the camera in the detector arm was 47 kHz. The resolution was 8 μm (in air) depthwise and 13 μm laterally; 512 × 512 pixels with 512 frames were used to construct a 3D image with the Amira program (Visage Imaging, Inc. San Diego, CA).

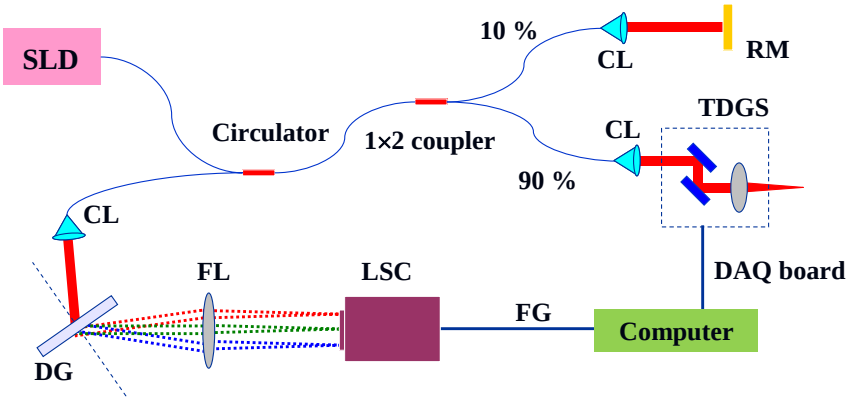

Figure S1. Schematic of high-speed SD-OCT. CL: Collimating Lens; DG: Diffraction Grating, FG; Frame Grabber, FL; Focusing Lens, LSC; Line Scan Camera, RM; Reference Mirror, SLD; Superluminescent Diode, TDGS; Two-Dimensional Galvo Scanner.

FT-IR spectroscopy

The chemical structures of SPDP-Au NP, KL-PEI, siRNA/KL-PEI polyplexes, and siRNA/KL-PEI-Au NP-PEG were compared using a Nicolet Magna 860 FT-IR spectrometer (Thermo Nicolet, Madison, WI). The solution of each sample in DI water was deposited on a calcium fluoride substrate and dried under vacuum for 12 h at room temperature. As shown in Figure S2 (blue line), SPDP shows the peaks at 1740 and 1575 cm^{-1}, corresponding to C=O (non-esteric) and C-C (aromatic) stretching of SPDP on the Au NPs, respectively. All the peaks were in agreement with a previous study showing the IR spectrum of SPDP on a gold-coated substrate [4]. Not all the peaks of SPDP were detected, possibly due to the orientation of the molecules on the gold where their dipole changes are parallel to the gold surface, resulting in infrared inactive vibrations (metal surface selection rule) [5]. For the spectrum of KL-PEI (green line in Figure S2), the strong bands observed at 1650 cm^{-1} and 1578 cm^{-1} are assigned to the C=O stretching and N-H bending of KL-PEI, respectively. The bands observed at 2850 - 2950 cm^{-1} (C-H stretching) are mainly attributed to methyl and methylene groups of KL-PEI. The spectra of siRNA/KL-PEI polyplexes (red line in Figure S2) showed almost similar peaks to those of KL-PEI, presumably due to a significantly higher amount of polymer than siRNA in the polyplexes prepared at an N/P ratio of 100. For the spectra of siRNA/KL-PEI-Au NP-PEG (black line in Figure S2), the peaks at around 3300 cm^{-1} (N-H stretching), 2920 cm^{-1} (C-H stretching), 1650 cm^{-1} (C=O stretching), and 1578 cm^{-1} (C-N stretching/N-H bending) that were mainly attributed to siRNA/KL-PEI polyplexes were clearly identified. Moreover, the intensity of peaks at 2920 and 2850 cm^{-1} was significantly increased compared to those of siRNA/KL-PEI polyplexes, mainly due to the conjugation of PEG which introduced -CH_2 groups.

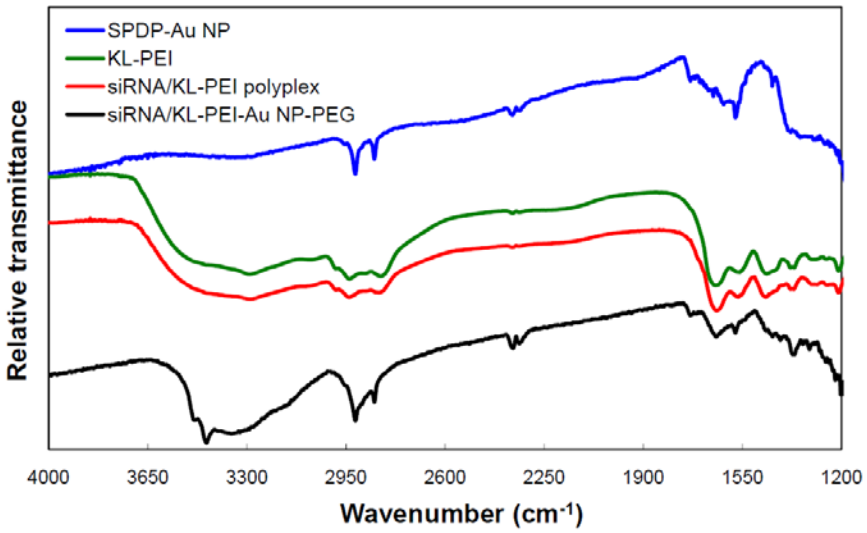

Figure S2. FT-IR spectra of SPDP-Au NP (blue), KL-PEI (green), siRNA/KL-PEI (red), and siRNA/KL-PEI-Au NP-PEG (black).

Quantification of Au NPs conjugated on siRNA/KL-PEI polyplexes by inductively coupled plasma optical emission spectrometry (ICP-OES)

ICP-OES was performed using a Perkin-Elmer Optima 7000 DV with Argon flow. siRNA/KL-PEI-Au NP-PEG nanoparticles prepared, as described in Experimental Section, were re-suspended in 960 μL of 0.1 M potassium cyanide (KCN) aqueous solution to ionize Au NPs. After 6 h at room temperature, the Au NP-dissolving solution was then diluted in a 2% HNO_3 matrix and the spectrum intensity of gold at 242.795 nm was measured. The amount of gold in a sample was determined by comparing the intensity with a calibration curve (1 to 100 ng gold/mL), which was obtained using a standard gold solution (1002 mg/L) (Sigma Aldrich, Milwaukee, WI). The number of gold atoms in the sample was then divided by the number of gold atoms per Au NP, in order to obtain the number of Au NPs. For a Au NP with a diameter of 15 nm, the number of gold atoms is estimated using the unit cell values of gold (4 atoms per cell; volume of unit cell = 0.0679 nm^3) and the volume of the Au NP, resulting in ~1.04×10^5 atoms per particle. The total gold amounts in the solutions dissolving SPDP-activated Au NPs and siRNA/KL-PEI-Au NP-PEG nanoparticles were compared to estimate a conjugation efficiency of SPDP-activated Au NP on the siRNA/KL-PEI polyplexes. Results shown in Table S1 indicate that 83% of SPDP-activated Au NPs were covalently immobilized on the siRNA/KL-PEI polyplexes, under the conditions used in this study.

Table S1. Quantified Au NPs before and after conjugation on the siRNA/KL-PEI polyplexes.

Sample	Gold concentration (μg/mL)	Au NP density (particles/mL)	Standard deviation (%)
Au NPs	4.5	1.3×10^{11}	2.9
SPDP-Au NPs	3.7	1.1×10^{11}	5.4
siRNA/KL-PEI-Au NP-PEG	3.1	9.0×10^{10}	5.4

Electrolyte concentration effects on zeta-potential changes

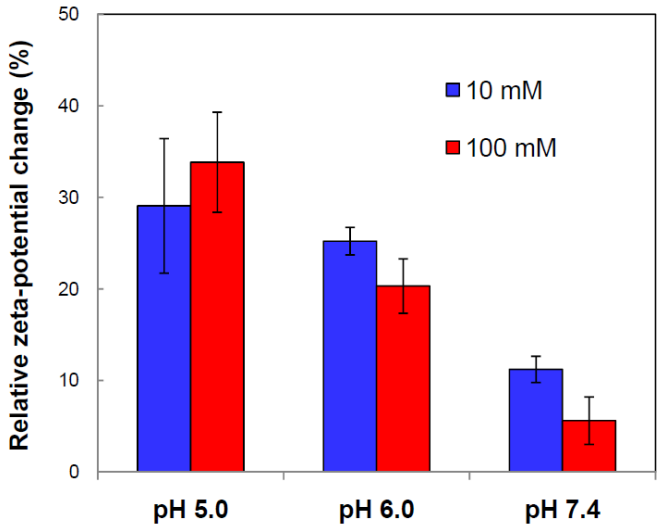

Figure S3. Effects of electrolyte concentration on zeta-potential changes of siRNA/KL-PEI-Au NP-PEG nanoparticles at various pHs. Acidic buffers (pH 5.0 and 6.0) were prepared by 10 and 100 mM acetic acid, and their pHs were adjusted by NaOH. The pH 7.4 buffer was prepared by 10 and 100 mM NaCl supplemented with 0.5 and 1.0 mM HEPES, respectively.

Cytotoxicity Assay

eGFP-expressing NIH 3T3 were inoculated at a density of 4×10^3 cells/well in a 96-well plate and incubated for 24 h. The culture medium was replaced with a mixture of a 4.8 μL aliquot of siRNA/KL-PEI-Au NP-PEG nanoparticle solution (15 pmol siRNA) and 70 μL of FBS-free DMEM, resulting in a final siRNA concentration of 200 nM per well. A 14.4 μL aliquot of pre-hydrolyzed siRNA/KL-PEI-Au NP-PEG nanoparticle solution (15 pmol siRNA) was added to the cells along with 60 μL of FBS-free DMEM. After 4 h of incubation, the medium was replaced with 100 μL of fresh DMEM containing 10% FBS. After the cells were further incubated for 24 h at 37°C, the medium was replaced with a mixture of 10 μL of 3-(4,5-dimethyl-2-thiazolyl)-2,5-diphenyltetrazolium bromide (MTT) (Sigma Aldrich, Milwaukee, WI) in PBS (10 mg/mL) and 90 μL of DMEM containing 10% FBS. After 3 h of incubation, the MTT solution was replaced with a mixture of 200 μL of DMSO and 20 μL of glycine buffer (0.1 M glycine, 0.1 M NaCl) to dissolve formazan precipitates formed by live cells. The relative viability of the cells was compared by UV absorbance at 561 nm. It was shown that Au NP conjugation and PEGylation lowered cytotoxicty of siRNA/KL-PEI-polyplexes by shielding the cationic surface, which was reversed when the shielded siRNA-carrying core was exposed after incubation at pH 5.0 for 10 min due to restored cationic surface charge (Figure S3).

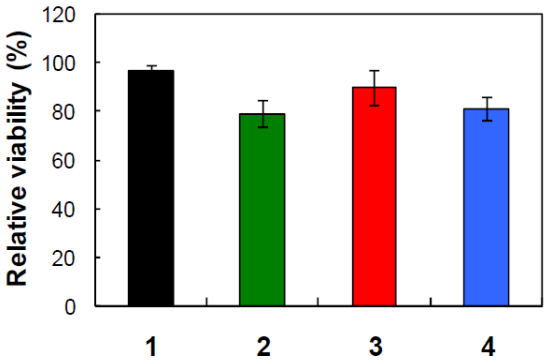

Figure S4. Cell viability of Au NP-conjugated polyplexes using eGFP-expressing NIH 3T3 cells at a siRNA concentration of 200 nM: **1**) Free Au NPs; **2**) siRNA/KL-PEI polyplex; **3**) siRNA/KL-PEI-Au NP-PEG nanoparticles; **4**) siRNA/KL-PEI-Au NP-PEG nanoparticles pre-incubated at pH 5.0 buffer for 10 min.

Quantification of eGFP gene silencing by flow cytometry

Experimental setup and siRNA/KL-PEI-Au NP-PEG nanoparticles for RNA interference test was prepared in the exactly same manner as described in the manuscript. eGFP-expressing NIH 3T3 cells were incubated with siRNA/KL-PEI-Au NP-PEG nanoparticles or pre-hydrolyzed (10 min) siRNA/KL-PEI-Au NP-PEG nanoparticles in serum-free medium at a final siRNA concentration of 200 nM in a well. After 4 h of incubation, the medium was replaced with fresh medium supplemented with 10% FBS. After a post 68 h-transfection incubation, the cells were harvested by trypsinization and washed with PBS for fluorescence analysis using a flow cytometer. The silencing of eGFP expression was quantified by mean fluorescence intensity of the cell incubated with the siRNA/KL-PEI-Au NP-PEG nanoparticles in comparison with the cells incubated with media only.

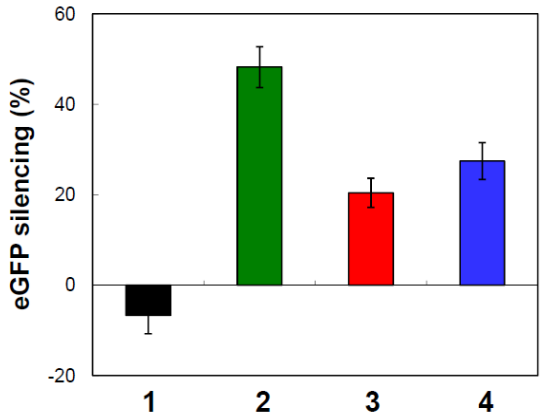

Figure S5. eGFP gene silencing efficiency (determined by flow cytometry) of: **1**) free Au NPs; **2**) siRNA/KL-PEI; **3**) siRNA/KL-PEI-Au NP-PEG without prior incubation at pH 5.0; **4**) siRNA/KL-PEI-Au NP-PEG incubated at pH 5.0 for 10 min.

siRNA concentration-dependent gene silencing and cytotoxicity

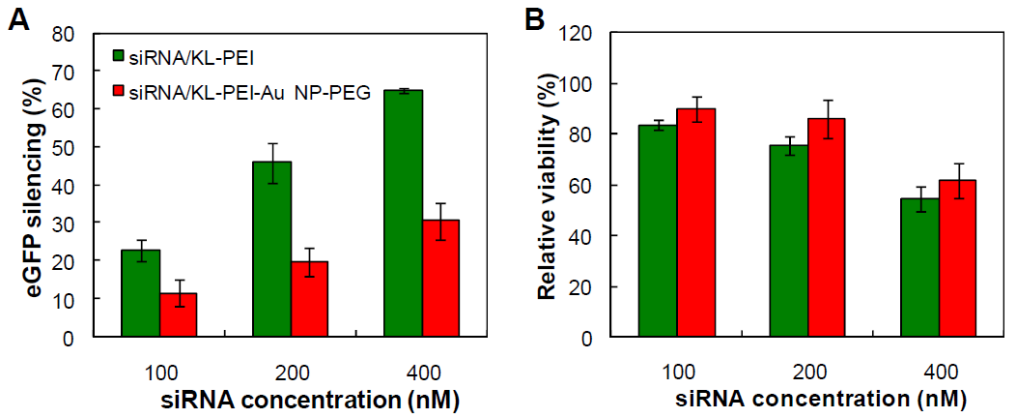

Figure S6. (A) eGFP silencing and (B) relative viability of eGFP-expressing NIH 3T3 cells incubated with siRNA/KL-PEI-Au NP-PEG nanoparticles at various siRNA concentrations. eGFP-expressing NIH 3T3 cells were incubated with nanoparticles in serum-free medium for 4 h followed by post 68 h-transfection incubation with fresh medium supplemented with 10% FBS. Cell viability was measured by a conventional MTT assay as described above. It was clearly shown that gene silencing efficiency and cell toxicity by siRNA/KL-PEI-Au NP-PEG nanoparticles were increased with siRNA concentration.

Optimized incubation time at an acidic pH for gene silencing

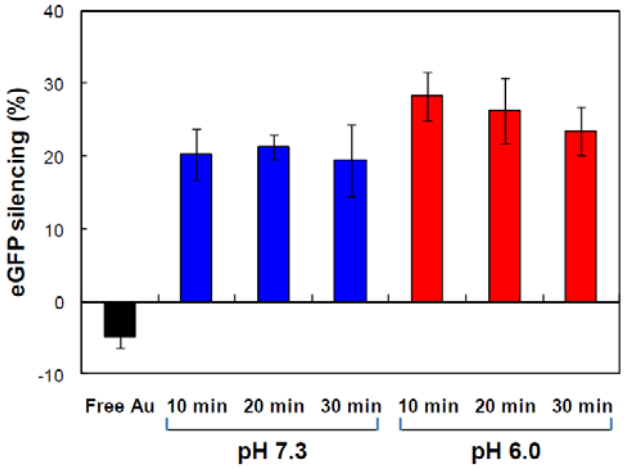

Figure S7. In vitro gene silencing efficiency by siRNA/KL-PEI-Au NP-PEG nanoparticles in a normal tissue (pH 7.3) and a mildly acidic tumor environment (pH 6.0), determined by flow cytometry. eGFP-expressing NIH 3T3 cells were incubated with siRNA/KL-PEI-Au NP-PEG nanoparticles for different periods of time (e.g., 10, 20, and 30 min) at pH 7.3 and pH 6.0 serum-free DMEM, followed by 4 h-transfection at pH 7.3. A final siRNA concentration was adjusted to 200 nM in a well. eGFP silencing efficiency was quantified after post-transfection incubation for 68 h in 10% FBS-containing medium.

REFERENCES

[1] Kasai, C.; Namekawa, K.; Koyano, A.; Omoto, R. IEEE *Transactions on Sonics and Ultrasonics* **1985**, *SU-32*, 458-464.

[2] Wang, L.; Wang, Y.; Guo, S.; Zhang, J.; Bachman, M.; Li, G.; Chen, Z. *Opt. Commun.* **2004**, *242*, 345-350.

[3] Ahn, Y.-C.; Jung, W.; Chen, Z. *Lab Chip*. **2008**, *8*, 125-133.

[4] Ferretti, S.; Paynter, S.; Russell, D. A.; Sapsford, K. E.; Richardson, D. J. *Trends Anal. Chem*. **2000**, *19*, 530-540.

[5] Hayden, B. E. In *Vibrational Spectroscopy of Molecules on Surfaces*; Yates, J. T., Madey, T. E.; Plenum: New York, 1987, p 267.